DOI: 10.24874/ti.1741.08.24.10

Tribology in Industry

www.tribology.rs

RESEARCH

Effect of Plasma Quenching Parameters on Hardened Layer Properties in Railroad Wheels

Azamat Kanayev[a,*], Amangeldy Kanayev[b] and Aliya Moldakhmetova[c]

[a]*Department of Scientific Projects and Publications, L. Gumiliyov Eurasian National University, 2 Satbayev St., Astana, Kazakhstan,*
[b]*Department of Standardization, Certification and Metrology, L. Gumiliyov Eurasian National University, 2 Satbayev St., Astana, Kazakhstan,*
[c]*Department of Scientific Projects and Publications, L. Gumiliyov Eurasian National University, 2 Satbayev St., Astana, Kazakhstan.*

Keywords:

Surface hardening
Plasma selective quenching
Railroad wheels
Structure
Mechanical properties
Wear resistance
Rotation frequency

* Corresponding author:

Azamat Kanayev
E-mail: kanayev_a@outlook.com

Received: 27 August 2024
Revised: 8 October 2024
Accepted: 3 December2024

A B S T R A C T

This research investigates the effect of quenching current, nozzle-to-surface distance, plasma-forming gas flow rate, and rate of cooling on both plasma torch travel speed (treatment speed) and nozzle diameter. Cooling rates were calculated for various quenching currents based on heat transfer theory. Results show that the relative significance of primary plasma selective quenching parameters remains consistent for both hardened zone depth and width. Notably, the effect of quenching current on hardened zone depth significantly exceeds that of other parameters, highlighting its critical role for optimizing railroad wheel performance. We propose a novel method for controlling the mechanical properties of the hardened surface through regulating wheelset rotational speed during quenching. This approach has the potential to significantly improve the wear resistance and lifespan of railroad wheels, leading to substantial cost savings for the railway industry.

1. INTRODUCTION

Surface hardening techniques utilizing concentrated energy flow, such as laser, plasma, electron beam, and cathode ions, have seen notable advancements. Among these, plasma selective quenching emerges as a distinctive method characterized by its cost-effectiveness, equipment accessibility, environmental friendliness, and operational efficiency. It boasts larger dimensions (both depth and width) of the hardened zone, making it an attractive option for industrial applications. Importantly, these advantages seamlessly integrate into standard production facilities, with surface plasma treatment proving

technically more accessible than conventional volumetric and surface heat treatment methods.

The essence of plasma processing lies in the ultra-fast heating of the metal surface through a plasma arc, followed by rapid cooling due to heat transfer to the inner layers of the product. This unique approach to forced cooling, accomplished without the need for a coolant on the heated surface, significantly streamlines the thermal hardening process [1-2].

The quenching process induces ultrafast cooling of the workpiece, attributed to the localized nature of plasma heating, which stands in contrast to conventional heating techniques. It is noteworthy that localized heat treatment, both technically and economically viable, focuses on hardening the heavily loaded working surface of products, therefore enhancing their wear resistance. Following plasma hardening, parts exhibit a hardened surface layer typically reaching a depth of 1.0-1.5 mm, often adequate for a substantial increase in wear resistance. Crucially, this hardening process seamlessly integrates into the heat treatment of wheels, proving highly productive. Note that, as a final stage of the process, it effectively enhances both the operational lifespan and service life of heavily loaded products without altering the overall elemental composition, physical and mechanical properties in the inner layers of the material [3-5].

Of practical interest is the investigation into the controlled modification of railway wheel rim surface properties (primarily hardness) to achieve desired performance characteristics. Experiments have shown that this is achieved through a novel rotation mechanism, developed by the authors, which provides the required wheelset rotation speed during plasma selective quenching [6].

2. MATERIALS AND RESEARCH METHODS

The object of research is a solid-rolled railroad wheel made of carbon structural steel with the following elemental composition, %: 0.44-0.52 C, 0.80-1.20 Mn, 0.40– 0.60 Si, 0.08 - 0.15 V, not more than 0.035 P (GOST 10791-2011). There is evidence that higher carbon (according to GOST) provides the necessary wear resistance and contact resistance (crack resistance) on the one hand but reduces heat resistance on the other. Current carbon steel does not fully meet the demands of future wheel operating conditions. Consequently, 65F steel has been developed for freight wagons and 45GSF steel for high-speed passenger train wheels. The addition of vanadium (denoted by "F" in grades) improves wear resistance, fracture toughness, and thermal stability compared to standard carbon steel.

We conducted our experiments using a certified UDGZ-200 mobile plasma torch, which provides non-contact arc ignition, smooth arc current control, and gas purging before and after quenching [7,8].

An electrode with a rounded end and a ceramic plasma-forming nozzle (GOST 859-98) was used to quench the surface layer of the wheel. The device is equipped with a flow controller for plasma-forming gas with an AR-40 flow indicator, which lowers the pressure of the gas flowing from the tank and automatically maintains a constant set flow rate.

A plasma torch, operating within a current range of 220-250 A, facilitated the surface treatment process. This current range proved sufficient for effective treatment. Cooltec20™ served as the cooling fluid for the plasma torch, enhancing its operational lifespan. This enhancement stems from the fluid's neutral interaction with the processed material and its ability to significantly minimize scale deposition on the cooling system's inner surface.

Metallographic studies involved specimens prepared using a standardized technique, effectively mitigating potential microstructural disturbances. Microstructural analysis, hardened layer depth measurement, and microhardness distribution across the hardened layer's cross-section were conducted using a PMT-3™ hardness tester. A Neophot-31™ optical microscope facilitated microscopic examination of meticulously prepared cross-sectional specimens. This meticulous preparation ensured the preservation of the hardened layer throughout the analysis [9,10].

In this work, argon of a normal purification grade (GOST 10157-93) was used as the plasma-forming gas, considering the cost, the conditions of chemical interaction with the processed material (inertia), the operating voltage of the arc, and the heat content and temperature.

The presented results are averaged from a series of five experiments, with mean values used from these five experiments. Statistical criteria are expressed through calculated probability and significance level, so the accuracy and reliability of the measurements were estimated using a confidence interval calculated by the formula $p = 1-\alpha$, where p is the calculated probability (p value) and α is the significance level. In our calculations, we used p=95% and α=0.05, meaning that only 5% of the measurements may contain some errors [11,12].

3. RESULTS AND DISCUSSION

The main parameters of the plasma treatment include, in addition to the flow of plasma-forming gas, the current, nozzle-to-surface of the quenched product, the speed of the plasma torch movement at different diameters of the ceramic nozzle [13-15].

The study of the influence of plasma hardening parameters on the depth (h) and width (b) revealed the following.

The relationship between the depth and width of the quenched zone and the process parameters at d_n=3.8 mm and s=20 mm is described by formulas (1) and (2).

$$\frac{\Delta h}{h} = 3.58\frac{\Delta I}{I}+0.6\frac{\Delta G_p}{G_p}+0.4\frac{\Delta l}{l}-0.16\frac{\Delta \upsilon}{\upsilon} \quad (1)$$

$$\frac{\Delta b}{b} = 1.83\frac{\Delta I}{I}+0.34\frac{\Delta G_p}{G_p}+0.21\frac{\Delta l}{l}-0.07\frac{\Delta \upsilon}{\upsilon} \quad (2)$$

where $\Delta I/I$ is the effect of the plasma arc current.
$\Delta G_p/G_p$ is the flow rate of the plasma-forming gas.
Δl/l is the distance between the nozzle and the surface of the product.
$\Delta \upsilon/\upsilon$ is the speed of the plasma torch (processing speed).
d_n is the diameter of the ceramic nozzle.
s is the distance between the nozzle cutoff and the treated surface.

These formulas are derived from previous research [16], show that the process parameters effect hardened zone depth and width similarly, in decreasing order of effect: constricted arc current, plasma gas flow rate, nozzle-to-workpiece distance, and movement speed (for a constant nozzle diameter).

The originality of these experimental studies is based on the effect of the constricted arc current on the dimensions of the plasma selective quenching zone is significantly stronger than the influence of other process parameters. Therefore, the arc current may serve as the primary control parameter for the plasma selective quenching.

A critical analysis of literature data shows that two external factors must be considered when choosing the depth and width of the hardened layer during plasma selective quenching:

First, the heating temperature at each quenching point should be equal to or greater than the critical temperature for that material $T_h \geq T_q$ (T_q = 850°C, GOST 10791-2011 for wheel steel).
Secondly, the processing rate at each point must be at least the critical quenching rate in water to obtain a martensitic structure [17-20].

Experiments revealed that, to prevent excessive grain growth and surface melting, the maximum metal temperature during quenching should be limited (to 1100-1200°C for wheel steel). It is important to distinguish these temperatures from the quenching temperature (T_q = 850°C); they are provided solely to emphasize that the surface temperature of the wheel steel should remain below these limits during quenching.

Table 1 shows the effect of the current in the range from 60 A to 200 A on the processing speed υ (m/h) and the line energy q (J/mm) for d_n = 3.0 mm, s = 20 mm and to keep track the patterns in the chart (Figure 1).

Table 1. Dependence of the processing speed and the line energy on the current.

N	I (A) at d_n=3 mm, s = 20 mm									
1	I (A)	60	70	80	100	120	140	160	180	200
2	v (m/h)	100	120	70	42	30	21	17	13	11
3	q (J/mm)	30	34	90	200	305	420	550	690	840

Figure 1 illustrates the relationship between travel speed υ (m/h), line energy q (J/mm), and constricted arc current within the range of 60-200 A at plasma selective quenching, (d_n = 3.0 mm, s = 20 mm).

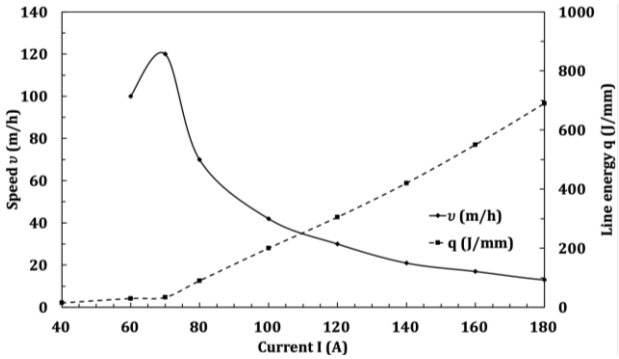

Fig. 1. Dependence of travel speed and line energy on constricted arc current during plasma hardening (d_n= 3.0 mm and s = 20 mm).

In practice, the processing speed (movement of the plasma torch) is of great importance because it determines the performance of the hardening and the line energy that affects the degree of thermal deformation of the product. Experiments have shown that the speed of movement of the plasma torch must be reduced to prevent melting of the surface of the product. Thus, no melting of the surface was observed at a current of 140 A and below (processing speed of 21 m/h or 0.006 m/s). The line energy of above 420 J/mm, corresponding to the current of 140-200 A, leads to melting of the surface of the hardened part with its rough damage, accompanied by the formation of small drops of molten metal. This results in the need for cleaning to improve the market quality of the hardened surfaces [21-24].

Therefore, the obtained results show that the modes of plasma selective quenching without surface micromelting are in the range of υ = 21-100 m/h and q = 30-420 J/mm, respectively, in terms of processing speed and line energy.

In the other series of experiments, the effect of the plasma arc current and the diameter of the plasma nozzle (d_n=3.0 mm) at the distance from the nozzle to the hardened surface (s=20 mm) on the depth of the quenching zone was studied. Their results are presented in Table 2.

Table 2. Dependence of the quenching zone depth on the arc current.

N	**I (A) at d_n=3 mm, s = 20 mm**									
1	I (A)	60	67	80	95	115	140	160	180	200
2	h (mm)	0.4	0.92	1.00	0.9	0.77	0.66	0.60	0.52	0.43

The data analysis presented in Table 2 reveals that, within the quenching regime corresponding to arc currents of 50 A and above, the hardened layer depth increases from 0.06 mm to 1.0 mm at 80 A, and then gradually decreases to 0.43 mm at a quenching current of 200 A. (The plasma-forming nozzle diameter and the distance between the nozzle tip and the workpiece surface were maintained at constant throughout these experiments.)

As noted earlier, the current is the primary controllable parameter in the plasma selective quenching process, as its effect on the dimensions of the plasma-hardened zone is significantly greater than that of other plasma selective quenching parameters.

For structural steel 65G with the constant diameter of the plasma nozzle of 3 mm, the dependence of the hardening zone depth on the arc current is extreme. Two regions of possible modes of plasma selective quenching can be distinguished.

At relatively low arc currents (50-79 A) and slow travel speeds, the cooling rate of the metal limits the dimensions of the quenched zone. For 65G structural steel, a critical cooling rate of 100 K/s (373°C/s) is necessary to achieve a martensitic structure at the quenching temperature of 850°C. As previously noted, the workpiece surface temperature must remain below 1100-1200°C during quenching. This temperature range, below the melting point of the steel, avoids the need for subsequent grinding of the hardened surfaces.

At elevated plasma arc currents (above 80 A) and high travel speeds, the surface temperature of the workpiece becomes the limiting factor for hardened zone dimensions. This surface temperature must not exceed the predetermined maximum allowable value. Within this regime,

the cooling rate in the quenching zone exceeds the critical cooling rate required for martensitic transformation in this steel.

Note that the maximum value of the depth of the quenching zone (Table 2) corresponds to modes at the boundary between relatively low arc currents (60-67 A) and high plasma arc currents (above 80 A) and fast processing speeds. These results indicate that high currents are not advisable due to the formation of a shallow hardened zone.

The effect of plasma selective quenching current on the width of the hardened zone at d_n = 3.0 mm s = 20 mm is shown in Table 3. Note that the hardened zone depth is consistently denoted as h and the width as b.

Table 3. Dependence of the width of the quenching zone on the constricted arc current.

N	**I (A) at d_n=3 mm, s = 20 mm**									
1	I (A)	72	80	90	110	120	140	160	180	200
2	b (mm)	0.6	6.2	6.0	5.6	5.5	5.4	5.3	5.2	5.1

A comparative analysis of the data presented in Table 2 and Table 3 reveals that the trends in hardened zone depth and width as a function of arc current exhibit similar characteristics. In both cases, both the depth and width of the hardened zone decrease with increasing quenching current (depth from 0.9 mm to 0.43 mm, width from 5.6 mm to 5.1 mm). This similarity in the behavior of hardened zone width and depth with respect to both arc current and plasma-forming nozzle diameter (d_n = 3.0 mm), at a constant nozzle-to-workpiece distance (s = 20 mm) as shown in Tables 2 and 3, has practical implications for assessing the quality of the surface-hardened layer. This conclusion, drawn from the comparison of the data in Tables 2 and 3, is well-founded and obvious.

As is customary in the scientific and technical sources, when a plasma arc is sustained between an electrode and a workpiece, it is referred to as a "constricted arc." This terminology stems from the artificial confinement of the arc dimension by the walls of the plasma-forming nozzle, which leads to an increase in arc temperature. Consequently, a small nozzle diameter ensures the necessary arc constriction, thereby elevating the temperature. In addition to increasing the temperature, the confinement of the arc within the narrow ceramic nozzle enhances arc stability and increases the kinetic energy of the plasma jet [3,8].

Based on the results of the experiments, Table 4 presents the experimental values of cooling rates at a constant plasma arc voltage of 30 V, alternating arc currents of 100, 150, and 200 A, and arc travel speeds of 30 and 40 m/h (0.0083 and 0.0111 m/s, respectively).

Table 4. Experimental cooling rate φ (°C/s) as a function of plasma arc travel speeds of 30 and 40 m/h at current of 100, 150 and 200 A.

υ (m/h)	**υ (m/s)**	**φ (^{0}C/s) at I (A)**		
		100	150	200
30	0.0083	1035	1650	2230
40	0.0111	785	1190	1695

Comparison of the experimental cooling rates with the calculated values (Tables 4 and 8) demonstrates satisfactory agreement, with differences falling within the range of 7.4% to 15.5%. These results are therefore considered reliable. The calculated cooling rates are higher than the experimental ones, likely due to the rapid movement of the plasma arc.

Changing the diameter of the plasma-forming nozzle, which leads to a change in the effective radius of the plasma arc heat spot, results in an extreme change in the cooling rate (Table 5).

Table 5. Dependence of the cooling rate (υ) on the nozzle diameter (d_n).

N	d_n (mm) at I = 80 A, s = 10 mm								
1	Nozzle diameter d_n (mm)	2.4	2.5	2.6	2.8	3.0	3.4	3.6	4.0
2	Cooling rate υ (K/s)	1300	1090	750	600	400	210	160	110

It is evident that increasing the diameter of the plasma nozzle from 2.4 mm to 4.0 mm, while keeping the current (80 A) and the distance from the cut to the processed surface (10 mm) constant, results in a reduction in cooling rate from 1300 K/s to 110 K/s, which affects the depth and width of the hardened zone. This is likely due to changes in the degree of localization of the plasma treatment as the nozzle diameter decreases. Experimental results indicate that a plasma nozzle diameter of 2.8–3.0 mm ensures the critical quenching rate, leading to the formation of a martensitic structure, and is therefore considered optimal.

Utilizing a larger nozzle diameter effectively increases the hardened zone dimensions. For instance, employing a 4.0 mm diameter nozzle at a current of 110A yielded a hardened zone depth of 1.24 mm and a width of 7.94 mm. These values surpass those obtained using a 3.0 mm diameter nozzle at a current of 80A. Note that the workpiece thickness (*s*) remained constant throughout the experiments.

The data presented in Table 6 and Figure 2 demonstrate that a plasma nozzle diameter of 3.2 mm yields the largest hardened zone dimensions, achieving a maximum depth (*h*) of 1.1 mm and width (*b*) of 6.8 mm. Further increasing the nozzle diameter from 3.5 mm to 3.8 mm results in a sharp decrease in both the depth and width of the hardened zone, despite maintaining constant arc current and workpiece thickness.

Table 6. Dependence of the depth (h) and the width (b) of the quenching zone on the diameter (d_n) of the plasma-forming nozzle at I= 80 A, s =10 mm.

N	Dimen sions of the quenching zone	d_n (mm) at I= 80 A, s =10 mm								
		2.0	2.5	3.0	3.2	3.4	3.5	3.6	3.7	3.8
1	h (mm)	0.5	0.8	1.0	1.1	1.05	0.9	0.46	0.3	0.1
2	b (mm)	3.5	5.0	6.4	6.8	6.7	6.4	5.3	3.2	1.0

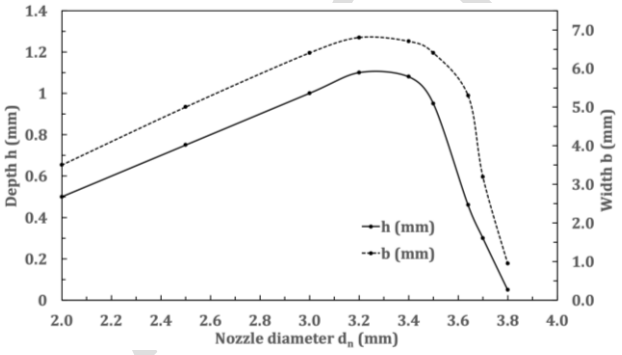

Fig. 2. Dependence of the depth (h) and the width (b) of the quenching zone on the diameter (d_n) of the plasma-forming nozzle at I= 80 A and s =10 mm.

As previously noted, the hardened layer depth is a more sensitive indicator of the quenching regime compared to the width of this zone.

The effect of the diameter of the plasma-forming nozzle d_n (mm) on the processing speed (the travel speed of the plasma torch) and the line energy of the plasma arc at I =80 A and s = 10 mm is shown in Table 7. As we can see the diameter of the plasma-forming nozzle has an opposite effect on the processing speed and the line energy of the plasma arc. Thus, when the diameter of the plasma-forming nozzle is increased from 2 mm to 4 mm, the processing speed (without surface micromelting) [25,26] decreases from 60 m/h to 3.6 m/h, while the line energy of the plasma arc increases continuously with an increase in the diameter of the plasma-forming nozzle in the specified range and reaches 1050 J/mm at a diameter of 4.0 mm.

Table 7. Dependence of the speed (υ) and the line energy (q) on the diameter of the plasma-forming nozzle (d_n) at I = 80 A, s = 10 mm.

N	Plasma quenching parame ters	d_n (mm) at I= 80 A, s =10 mm							
		2.0	2.5	3.0	3.3	3.5	3.8	3.9	4.0
1	υ (m/h)	60	25	12	8	6.7	5.0	4.8	4.7
2	q (J/mm)	50	140	300	490	615	790	860	1050

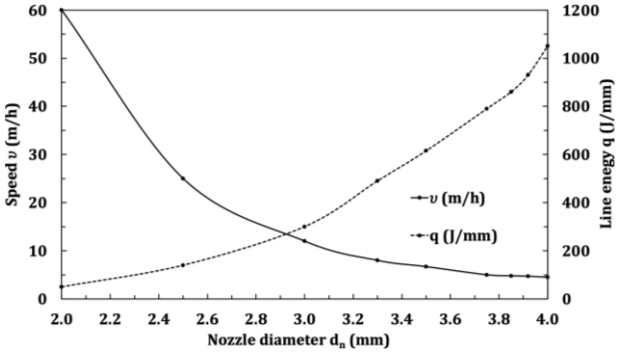

Fig. 3. Dependence of the speed of the movement and the line energy on the diameter of the plasma-forming nozzle (I =80 A and s = 10 mm).

These experimental results show the effect of the diameter of the plasma-forming nozzle on the processing speed and line energy, and the need to take these factors into account in developing the surface plasma processing of workpieces.

A comparative analysis was conducted to assess the experimentally determined cooling rates (ω, °C/s) of railroad wheels against theoretically calculated values. This analysis involved comparing these cooling rates with the processing rates observed during workpiece surface heating, employing operational parameters consistent with the UDGZ-200 plasma quenching system. The comparative study adhered to the established heat transfer theory developed by N.N. Rykalin [27,28].

Table 8 presents the calculated cooling rates. We have used the formula $\omega = q / (2 \pi \lambda \upsilon t^2)$ to calculate the cooling rates on the axis of movement of a strong point heat source in 1 s. after its passage. The power of the plasma arc is proportional to the current and the voltage drop across it. The voltage at quenching was not regulated. The other plasma treatment settings were chosen in the typical ranges for the UDGZ-200 plasma torch. The power of the plasma arc $q = IU$, the current varies in the range of 50-250 A, the coefficient of thermal conductivity of the steel λ is constant and is 47 W/(m°C) [29], the movement speed of the arc varies in the range of 5-40 m/h, the time is constant (1 s).

Table 8. Dependence of the calculated cooling rate on the travel speed of the plasma arc (quenching rate) at various current.

υ (m/h)	υ (m/s)	ω (^{0}C/s) at I (A)				
		50	100	150	200	250
5	0.0014	3631.96	7263.92	10895.88	14527.85	18159.81
10	0.0028	1815.98	3631.96	5447.94	7263.93	9079.91
20	0.0055	924.21	1848.43	2772.64	3696.86	4621.07
30	0.0083	612.24	1224.49	1836.73	2448.99	3061.22
40	0.0111	457.88	915.75	1373.63	1831.50	2289.38

We can see from the data shown in Table 8 and Table 4, the cooling rate (612.24-18159.81°C/c) for all current from 50 to 250 A exceed the critical quenching rate in water, which is ~500°C/c according to [20,29]. The exception is the cooling rate of 457.88°C/c for a plasma arc current of 50 A and its travel speed 0.0111 m/s.

A larger discrepancy between experimental and calculated cooling rates was observed at lower traverse speeds (5 m/h). As previously mentioned, the closer agreement at higher speeds is consistent with the analytical model's assumption of a rapidly moving heat source. Therefore, it can be asserted that, within the investigated range of amperage and plasma arc traverse speed (quenching speed),

the critical cooling rate required for plasma selective quenching is achieved across almost the entire parameter space at high-speed heating with a high-enthalpy plasma jet. Note that medium-carbon structural steels can be hardened at significantly lower cooling rates.

As noted earlier, the ability to control the mechanical properties of railway wheel surfaces to meet specific performance requirements is of significant practical interest. Extensive experimental investigations have validated the authors' novel mechanism for wheelset rotation control during plasma hardening, definitively achieving the desired microstructure and mechanical properties. [6,30]. This controlled rotation varies the contact time between the plasma jet and the railroad wheel surface, exerting a direct effect on the resulting microstructure, hardened zone depth, and microhardness distribution across the hardened surface layer.

Figure 4 illustrates the wheel quenching utilizing the wheelset rotation mechanism.

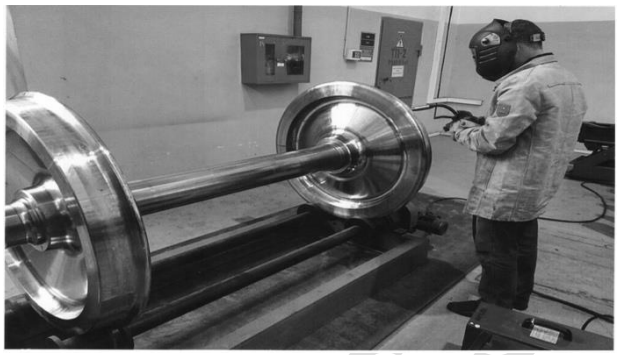

Fig. 4. Wheel Quenching with Wheelset Rotation.

Table 9 shows the effect of wheelset rotation speed on the hardened zone depth. As illustrated in Table 9, a rotation speed within the range of 0.150-0.160 rpm consistently produces a hardened structure with a depth of 0.5-1.2 mm.

Table 9. Test results of the wheel pairs by the rotation mechanism.

N	Wheelset rotation speed (rpm)	Microhardness on the surface (HV)	Quenching depth (mm)	Microstructure
1	0.170	1660	0.2-0.3	Lamellar martensite
2	0.160	1620	0.4-0.7	Martensite+bainite
3	0.150	1588	0.8-1.2	Troostite+Sorbite
4	0.145	1566	1.3-1.4	Sorbite+Pearlite
5	0.140	1529	1.5-1.7	Pearlite colonies
6	0.135	1449	1.8-1.9	Pearlite + ferrite

The test results according to the measured microhardness of the surface of the hardened layer (Table 9) show the controllability of mechanical properties of the railroad wheel by adjusting the rotation rate of the wheel pair.

Metallographic analysis, conducted using optical microscopy, reveals the formation of a heterogeneous gradient structure within the hardened surface zone – essentially creating a thin composite layer.

This unique microstructure enhances both wear resistance and fatigue strength, making the hardened steel significantly more resistant to crack initiation [31,32]. The originality of this research lies in uncovering this distinct microstructure and its profound impact on the material's mechanical performance.

4. CONCLUSIONS

1. This comprehensive investigation elucidates the multifaceted interplay of controllable factors governing the effective thermal power of a plasma arc. Significantly, the adaptability of plasma surface treatment extends beyond mere arc current adjustment. Factors encompassing plasma-forming nozzle diameter, treatment speed, plasma gas flow rate, quenching rate (which directly affects the hardened zone structure), and nozzle-to-workpiece distance exert critical, interrelated effects. The interconnected nature and mutual dependence of these factors of these factors is paramount when engineering plasma treatment technologies for high-load components, such as solid-rolled railroad wheels.

2. This research establishes a consistent effect of primary plasma selective quenching parameters on the resultant hardened zone dimensions (depth and width) across a range of plasma-forming nozzle diameters. Critically, the effect of arc current on the hardened zone dimensions supersedes that of other process parameters, highlighting its paramount importance as the primary controllable variable for achieving effective plasma hardening.
3. The calculation methodology employed herein, which assesses the cooling rate as a function of plasma arc movement speed (hardening rate), proves instrumental in determining the critical cooling rate required for effective plasma selective quenching. Notably, this methodology proves particularly robust in scenarios involving the ultrafast heating of railroad wheel rim treatments, encompassing a wide spectrum of processing parameters.
4. This study demonstrates the feasibility of achieving controlled and desirable mechanical properties in plasma-treated railroad wheel rims through the regulation of wheelset rotation speed during treatment. This assertion is substantiated by observed variations in microhardness, quenching depth, and steel microstructure as a function of wheelset rotation speed. This capability presents a practical avenue for tailoring the mechanical performance of treated surfaces to meet specific product or component requirements.

REFERENCES

[1] A.E. Balanovsky and V.T. Nguyen, "Increasing hardness of surface layer of Low-Carbon steel by account of plasma treatment of coating modification," Diffusion and Defect Data, Solid State Data. Part B, Solid State Phenomena/Solid State Phenomena, vol. 316, pp. 794–802, Apr. 2021, doi: 10.4028/www.scientific.net/ssp.316.794.

[2] V. Korzhyk, Y. Tyurin, and O. Kolisnichenko, *Surface modification of metal products by electrolyte plasma*, 2021. doi: 10.15587/978-617-7319-47-3.

[3] K. P. Hirpara, J. B. Valaki, M. D. Chaudhari, and M. A. Siddhpura, "A comprehensive review on recent developments in materials and technological parameters for plasma transferred arc hardfacing process," Proceedings of the Institution of Mechanical Engineers Part E Journal of Process Mechanical Engineering, vol. 238, no. 3, pp. 1507–1519, Feb. 2023, doi: 10.1177/09544089231153363.

[4] Y. Xiang, D. Yu, X. Cao, Y. Liu, and J. Yao, "Effects of thermal plasma surface hardening on wear and damage properties of rail steel," Proceedings of the Institution of Mechanical Engineers Part J Journal of Engineering Tribology, vol. 232, no. 7, pp. 787–796, Aug. 2017, doi: 10.1177/1350650117729073.

[5] J. Xu et al., "Investigation on wear and damage characteristics of high-speed rail steel with plasma selective quenching," Wear, vol. 486–487, p. 204100, Sep. 2021, doi: 10.1016/j.wear.2021.204100.

[6] A. Kanayev, A. Kanayev, and A. Moldakhmetova, "Ratio of Wheel/Rail Steel Hardness that Ensures Minimum Wear," Tribology in Industry, vol. 45, no. 3, pp. 408–415, Sep. 2023, doi: 10.24874/ti.1459.03.23.06.

[7] *Installation of plasma hardening UDGZ-200*. 2019.

[8] V.A. Korotkov, "SURFACE PLASMON HARDENING," Spravochnik Inzhenernyi Zhurnal, pp. 7–16, Jan. 2014, doi: 10.14489/hb.2014.12, pp.007-016.

[9] M.I. Boulos, P.L. Fauchais, and E. Pfender, Handbook of thermal plasmas. 2016. doi: 10.1007/978-3-319-12183-3.

[10] ASM Handbook vol. 8: Mechanical Testing and Evaluation, 10th ed., 2000.

[11] *Introduction to probability and statistics for engineers and scientists*. 2020. doi: 10.1016/c2018-0-02166-0.

[12] A. Kanaev, *Plasma selective quenching of heavy-duty parts and assemblies for transport engineering*, 2020.

[13] P.A. Topolyansky, S.N. Sharifullin, N.R. Adigamov, S.A. Ermakov, and A.P. Topolyansky, "Finished plasma strengthening and restoration of fuel equipment details," Journal of Physics Conference Series, vol. 1058, p. 012075, Jul. 2018, doi: 10.1088/1742-6596/1058/1/012075.

[14] P.G. Adischev, A.S. Tselischev, and M.V. Malkov, "*Research Trends in Development of New Wear Resistant Steel Grades*," Steel, no. 6, p. 54-57, Jun. 2021

[15] D.I. Weinboim, "*Energy Characteristics of an Arc Burning in Argon with Varying Degrees of*

Compression," Welding Production, no. 5, pp. 1-3, May 1984.

[16] P.A. Topolyansky and N.A. Sosnin, *"Hardening of Parts Using Arc and High-Frequency Plasma,"* Electrical Engineering Industry. Scientific and Technical Achievements and Advanced Experience, no. 1, pp. 24-27, Jan 1991

[17] K. Wang et al., "Study on the mechanism of plasma jet surface hardening of rail steels by using numerical method," Materials Today Communications, vol. 31, p. 103773, Jun. 2022, doi: 10.1016/j.mtcomm.2022.103773.

[18] X. Cao, C. Li, L. Chen, and B. Huang, "Experimental Study on the Design and Characteristics of a Laminar Plasma Torch with Medium Working Power and its Applications for Surface Hardening," IEEE Transactions on Plasma Science, vol. 48, no. 4, pp. 961–968, Mar. 2020, doi: 10.1109/tps.2020.2979411.

[19] D. Guo et al., "Laminar plasma jet surface hardening of the U75V rail steel: Insight into the hardening mechanism and control scheme," Surface and Coatings Technology, vol. 394, p. 125857, Apr. 2020, doi: 10.1016/j.surfcoat.2020.125857.

[20] G.E. Totten, Steel heat treatment. 2006. doi: 10.1201/nof0849384523.

[21] M. V. Zlokazov and V. A. Korotkov, "On practical application of plasma and laser hardening," Strengthening Technologies and Coatings, pp. 266–271, Jan. 2020, doi: 10.36652/1813-1336-2020-16-6-266-271.

[22] Y. Xiang, D. Yu, Q. Li, H. Peng, X. Cao, and J. Yao, "Effects of thermal plasma jet heat flux characteristics on surface hardening," Journal of Materials Processing Technology, vol. 226, pp. 238–246, Jul. 2015, doi: 10.1016/j.jmatprotec.2015.07.022.

[23] C. Fang et al., "Analyses on the nonequilibrium transport processes in a free-burning argon arc plasma under different operating conditions," Plasma Sources Science and Technology, vol. 31, no. 1, p. 015015, Oct. 2021, doi: 10.1088/1361-6595/ac2c8d.

[24] J. Nikolaou, L. Bourithis, and G. Papadimitriou, "Selective Case Hardening of Plain Steel by Carbon Alloying with a Plasma Transferred Arc (PTA) Technique," Journal of Materials Science, vol. 38, no. 13, pp. 2883–2891, Jan. 2003, doi: 10.1023/a:1024492720694.

[25] V. A. Korotkov, S. P. Anan'ev, and A. V. Shekurov, "Investigation of the effect of the cooling rate on the quality of the surface layer in plasma quenching," Welding International, vol. 27, no. 5, pp. 407–410, Oct. 2012, doi: 10.1080/09507116.2012.715926.

[26] J. Yu, H. Zhou, L. Zhang, L. Lu, and D. Lu, "Microstructure and properties of modified layer on the 65MN steel surface by Pulse Detonation-Plasma Technology," Journal of Materials Engineering and Performance, vol. 31, no. 2, pp. 1562–1572, Sep. 2021, doi: 10.1007/s11665-021-06258-2.

[27] N.N. Rykalin, *Calculation of thermal processes during welding*, 1951.

[28] N.N. Rykalin, A.V. Nikolaev, and A.N. Assonov, "Energy characteristics of an arc plasma torch in pulsed mode," in Physics, Technology, and Application of Low-temperature Plasma, Alma-Ata, pp. 500-504, 1990,

[29] G. Woan, The Cambridge Handbook of Physics Formulas. 2000. doi: 10.1017/cbo9780511755828.

[30] A. Kanaev, D. Orynbekov, "*Gradient Layer Structure Formation During Plasma Treatment of Wheel Steel,"* International Journal of Mechanical and Production Engineering Research and Development", vol. 10, no. 3, pp. 457-466, Mar. 2020.

[31] A.V. Bogomolov, A.T. Kanaev, and T.E. Sarsembaeva, "Determination of mechanical characteristics plasma hardened wheel steel," IOP Conference Series Materials Science and Engineering, vol. 969, no. 1, p. 012037, Nov. 2020, doi: 10.1088/1757-899x/969/1/012037.

[32] A.V. Brover and G.I. Brover, *"Improving the Quality of Coatings Deposited on the Surface of Steels by Electrospark Alloying and Ion-Plasma Sputtering Using Laser Treatment,"* Hardening Technologies and Coatings, vol. 13. no. 10., pp. 442-446, Oct. 2017.